

Oxidation in the γ Phase of Spinel Containing Iron II: Influence of Defects on the Oxidation Kinetics and Electrical Properties

B. GILLOT*

*Laboratoire de Recherches sur la Réactivité des Solides associé au CNRS
Faculté des Sciences Mirande, B.P. 138, 21004 Dijon Cedex, France*

F. CHASSAGNEUX

*Laboratoire de Chimie Minérale, Université Claude Bernard, Lyon I, 43
boulevard du 11 Novembre 1918, 69621 Villeurbanne, France*

AND A. ROUSSET

*Laboratoire de Chimie des Matériaux Inorganiques, Université Paul
Sabatier, Toulouse III, 118, route de Narbonne, 31000 Toulouse, France*

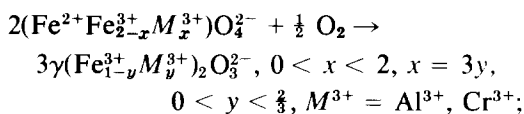
Received July 8, 1980; in revised form December 5, 1980

After a review of the distribution of vacancies in defect phases resulting from $\gamma\text{Fe}_2\text{O}_3$, the authors give several examples drawn from oxidation kinetics and electrical properties, where the vacancies play a basic part due to their concentration as well as their location. The decrease in chemical diffusion coefficient with increase in vacancy extent and the variation of the exponent from the pressure law with the extent of association are dependent on concentration, while the nature of the electron hopping between Fe^{2+} and Fe^{3+} ions is governed by the location of vacancies in the two types of sites in the spinel lattice.

Introduction

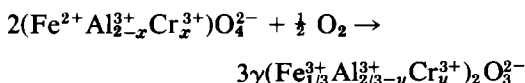
Over the last few years our laboratory has investigated mixed oxides of spinel structure containing iron II. The phases, prepared at relatively low temperatures (from 300°C), are very finely divided and thus are highly reactive with oxygen. If total oxidation of Fe^{2+} ions can be achieved below 400°C, which requires crystallites of less than 3000 Å, as we have shown with Dupré and Rousset (1), the oxidation reaction is topotactic and the oxygen lattice is

preserved. In such cases it leads to defect spinels (2-5), most of which are new combinations. These phases are derived from $\gamma\text{Fe}_2\text{O}_3$ either through the substitution of Fe^{3+} ions by trivalent ions such as Al^{3+} or Cr^{3+} or through the simultaneous substitution of Fe^{3+} ions and vacancies by divalent ions such as Zn^{2+} , Ni^{2+} , Co^{2+} , etc. In the former case the oxidation reactions of the type:

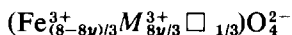


* To whom correspondence should be addressed.

and



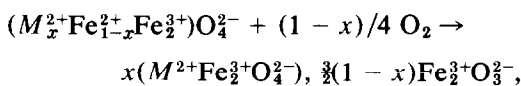
result in defect phases whose structural formulas may be written as



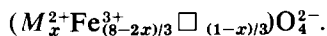
and



In the latter case the oxidation reaction is written:



and the defect phase may be written as



After reviewing the different methods used to express the location of vacancies and their possible ordering on the octahedral and tetrahedral sites of the spinel lattice, we show how they affect, through oxidation, the kinetic and electrical behavior.

Samples and Experimental Methods

The techniques of preparation and characterization (DTA, X-ray analysis, specific area, chemical analysis, morphology) have already been published in Refs. (6-8). The particle size of samples prepared at 700°C is less than 1000 Å (500-700 Å). Moreover, the particle mean diameter deduced from specific surface area measurement (between 23 and 35 m²/g) is in a good accordance with that obtained by means of electron microscopy and X-ray diffraction.

X-Ray analysis and magnetic measurements (3) were used to determine the distribution of vacancies vs substitution extent x and vs oxidation extent α . The effect of substitution and conversion ratio on the formation of vacancy-ordered superstructure has been investigated using ir spec-

troscopy (measurements *in situ*) and X-ray diffraction (9). Partial oxidations were achieved using a thermobalance and by halting the reaction by cooling and pumping. α is then determined by the ratio of the weight gains corresponding to desirable partial oxidation to total oxidation of all the Fe²⁺ ions.

Although oxidations in lacunar γ phases occur at relatively low temperatures and pressures (less than 250°C and 0.016 atm, respectively, for slightly substituted magnetites), these must still be lowered to obtain a better low-intensity-ray resolution in X-ray diffraction (9). Indeed, the longer the reaction, the better resolved the low-intensity rays, which may be explained by a better crystallization of the material and a better homogenization of vacancy distribution throughout the grain. Thus for each conversion rate α , reaction times of 24 hr and more were used, effecting oxidations at temperatures of about 150°C and oxygen pressures of about 10⁻⁷ atm. Under low oxygen pressure, the oxidation kinetic was found to be governed by the surface reaction and it is possible to obtain partially oxidized phases of uniform composition (10).

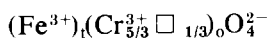
The dc conductivity was measured by means of four-probe and two-probe methods on compressed, sintered pellets of about 0.8 cm diameter and 0.2 cm thickness; both techniques gave identical results (11). For this study the influence of grain size on electrical conductivity has not been considered but such an influence has been reported in Ref. (11).

Position of Vacancies in γ Metastables Phases Totally Oxidized and during Oxidation

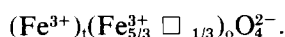
1. Position of Vacancies in Totally Oxidized γ Phases

The evolution of the lattice parameter of

$\gamma(\text{Fe}_{1-y}\text{Cr}_y)_2\text{O}_3^{2-}$ cubic phases $0 < y < 0.625$ vs their composition (Fig. 1) is explained assuming a progressive substitution of iron by chromium on the octahedral sites of $\gamma\text{Fe}_2\text{O}_3$, which requires the vacancies to be on those sites where they were generated (3). Thus we can deduce the structural formula of the defect spinel of composition $y = 0.625$ from that of $\gamma\text{Fe}_2\text{O}_3$ through substitution of Fe^{3+} ions by Cr^{3+} ions, which gives:



and



This distribution is confirmed by calculating the dimensions of such crystal lattices using the Poix method (12) (Fig. 1), which considers that the parameter of a crystal cell in an ionic oxide depends on the cation-oxygen distances.

Another proof of the fact that vacancies remain on octahedral sites is given by the magnetic study of these compounds (3) comparing the experimental value of the magnetic moment at saturation measured at 4.2°K with the value theoretically calculated following the ferrimagnetism model

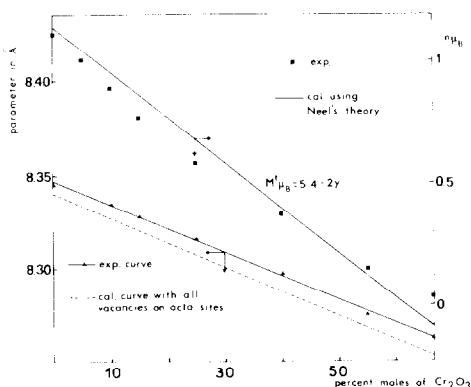


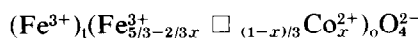
FIG. 1. Variation in the lattice parameter and magnetic moments at saturation of solid solutions $\gamma(\text{Fe}_{1-y}\text{Cr}_y)_2\text{O}_3$.

with two sublattices of Néel. Figure 1 shows that the agreement is satisfactory.

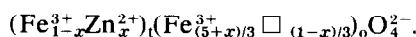
One should mention that in the case of nonstoichiometric magnetite at high temperature this distribution changes, vacancies would be distributed on both kinds of cationic sites (13). Moreover, the effect of particle size on distribution and ordering of vacancies in the sesquioxide $\gamma\text{Fe}_2\text{O}_3$ is discussed in Ref. (9). It has thus been shown that vacancies are only partially ordered for fully oxidized magnetite samples whose crystallite size is about 100 Å.

For higher substitution extents, such as the defect compound resulting from the oxidation of $(\text{Fe}^{2+}\text{Fe}_{2-x}^{3+}\text{M}_x^{3+})\text{O}_4^{2-}$ with $x > 1.87$ or defect compounds of type $(\text{Fe}_{8/9}^{3+}\text{Al}_{16/9-8/3y}^{3+}\text{Cr}_{8/3y}^{3+} \square_{1/3})\text{O}_4^{2-}$ obtained by oxidation of iron II chromialuminates we must expect the existence of vacancies on tetrahedral sites. Using the data deduced from the lattice parameter utilizing the invariant method of Poix (14) we find a distribution of vacancies in the amount of $\frac{1}{9}$ on tetrahedral sites and $\frac{2}{9}$ on octahedral sites, which may be written as $(\text{Fe}_{8/9}^{3+} \square_{1/9})_t(\text{Al}_{16/9-8/3y}^{3+}\text{Cr}_{8/3y}^{3+} \square_{2/9})_o\text{O}_4^{2-}$.

Another case where the determination of the lattice parameter and magnetic measurements allowed the location of vacancies is given by the oxidation of magnetites substituted by divalent ions. The replacement of Fe^{3+} ions and of vacancies by cobalt in $\gamma\text{Fe}_2\text{O}_3$ occurs only on octahedral sites (2), whereas replacement by zinc occurs on tetrahedral sites (5) yielding the two following formulas:



and



By analogy with $\gamma\text{Fe}_2\text{O}_3$, we may also expect, at least for compounds with vacancies only on octahedral sites, some ordering of the vacancies. In a recent study using ir spectrometry and X-ray diffraction we have

actually shown (9) that the vacancies were ordered on octahedral sites in the defect phases derived from $\gamma\text{Fe}_2\text{O}_3$, provided, however, that these phases were either slightly substituted by trivalent ions or slightly substituted by divalent ions. However, besides the characterization of γ phases, the determination, during oxidation, of the location and ordering of vacancies is also of interest as it allows one to define the spinel during its formation, i.e., its usual conditions of kinetic study and electrical behavior.

2. Location of Vacancies during Oxidation

The lattice parameter vs transformation extent α was found to decrease linearly for all the samples (Fig. 2). In addition, the experimental values obtained are in good agreement with the theoretical values calculated considering that during oxidation the vacancies are distributed in the same way as for totally oxidized products (Fig. 2). The ir spectra recorded for various transformation extents confirm these results (Fig. 3). They evolve continuously with α whether the vacancies are ordered or not. In the former case, occurring solely for low substitution extents ($x < 0.25$), the ir spectrum for $\alpha > 0.76$ shows a relatively large number of absorption bands in the region 200–700 cm^{-1} (Fig. 3), while the X-ray diffraction shows superstructure rays.

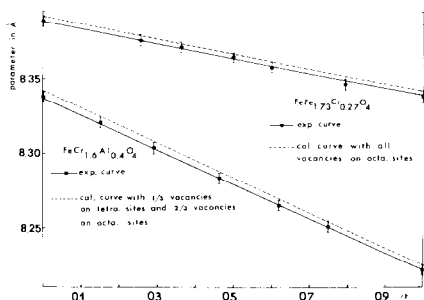


FIG. 2. Variation in the lattice parameter with the oxidation extent α .

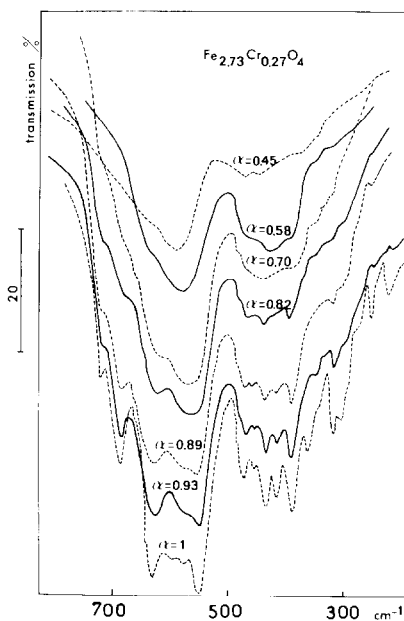


FIG. 3. Evolution of infrared spectra of chromium-substituted magnetite ($x = 0.27$) with oxidation extent α .

For $\alpha < 0.70$ the number of absorption bands decreases progressively, and for $\alpha = 0$ only two specific diffuse bands of inverse spinels remain. For higher substitution extents ($x > 0.80$) the small number of absorption bands and the absence of superstructure rays in the X-ray diffraction patterns whatever α excludes any vacancy ordering on octahedral sites.

These few examples which enabled us to define the location and the ordering of vacancies in γ phases, whatever the substitution extent of the spinel, show that the oxidation reaction may be considered as perfectly homogeneous with as a mere consequence a change in stoichiometry.

However, contrary to most nonstoichiometric oxides such as $\text{Ni}_{1-\delta}\text{O}$, $\text{Co}_{1-\delta}\text{O}$, $\text{Fe}_{1-\delta}\text{O}$ (15, 16), or even $\text{Fe}_{3-\delta}\text{O}_4$ at high temperature (17, 18), the deviation from stoichiometry is large since for totally oxidized γ phases written as $(\text{FeM}_2)_{1-\delta}\text{O}_4$, δ is equal to 0.33 ($\delta = \alpha/3$), whereas in binaries it is usually only a few percent. Let us note,

however, that for partially oxidized magnetites or for magnetites substituted by divalent ions δ may be lower since in the latter case it is for instance equal to $(1 - x)/3$.

Influence of Defects on Oxidation Kinetics

1. Decrease in Chemical Diffusion Coefficient with Vacancy Extent

The oxidation kinetics investigated over the temperature range 150–450°C and for pressures between 10^{-4} to 10^{-1} atm have been interpreted by the diffusion law, in variable working conditions, of the vacancies generated at the solid–gas interface (19). Indeed the experimental curves $\alpha = f(t)$ are identified with a theoretical diffusion curve whose expression for a sphere is written as:

$$\alpha = 1 - \frac{6}{\pi^2} \sum_{n=1}^{\infty} \frac{1}{n^2} e^{-n^2 kt},$$

with $k = \pi^2 \bar{D} / r^2$,

where r is the grain mean radius and \bar{D} the chemical diffusion coefficient. For sufficiently long oxidation times ($\alpha > 0.30$), this equation, for \bar{D} constant, may be written:

$$\log(1 - \alpha) = \log 6/\pi^2 - kt = f(t)$$

and \bar{D} can be determined directly from the slope of $\log(1 - \alpha) = f(t)$. Figure 4 shows the transforms for some spinels substituted by trivalent ions and Fig. 5 relates to zinc-substituted magnetites. For all these spinels, apart from the spinel strongly substituted by zinc ($x = 0.76$), the chemical diffusion coefficient is no longer constant. From a transformation extent $\alpha > 0.70$, it decreases with α , i.e., with increase of the vacancy number. But for the spinel substituted by zinc of composition $x = 0.76$, \bar{D} is constant for any α ; in this case the number of vacancies is not large since it is directly

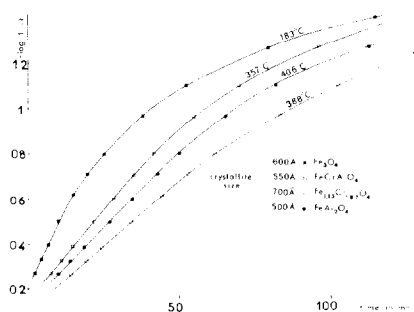


FIG. 4. Transformed curves $\log(1 - \alpha) = f(t)$ for spinels substituted by trivalent ions.

related to the number of Fe^{2+} ions initially present.

The decrease of \bar{D} when deviation from stoichiometry rises, also observed by Gallagher *et al.* (20) in the oxidation of pure magnetite and by other authors (21, 22) during the reduction of some simple oxides such as FeO and MnO, has been attributed to an increase in the energetic interactions of vacancies—electron holes (or in other words, to vacancy– Fe^{3+} interactions), which generate complexes consisting of dipolar pairs. It should also be noted that given the relatively low temperature where these defects occur, the phenomena of association are more important than at higher temperatures when usually the defects are generated in oxides (between 900 and 1300°C). This association phenomenon is confirmed by the exponent of the pressure law.

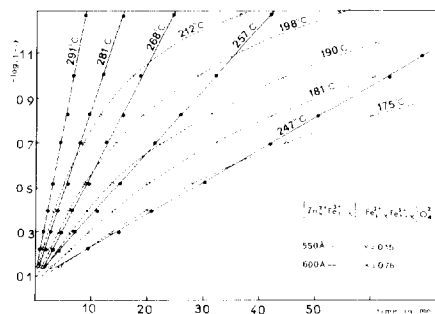
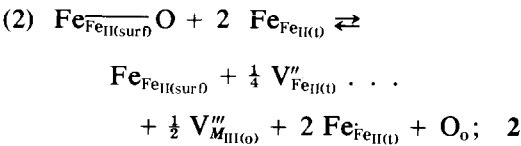
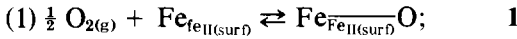


FIG. 5. Transformed curves $\log(1 - \alpha) = f(t)$ for zinc-substituted magnetites.

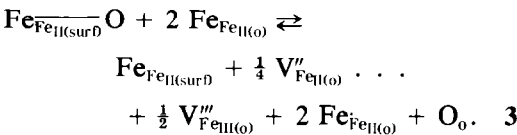
2. Variation of the Pressure Law Exponent with the Extent of Association

Using Kröger and Vingt's notation (23) we have already shown (24) that the elementary steps in the oxidation of a direct spinel to the γ phase, including both the interfacial and diffusion steps will be expressed as follows:

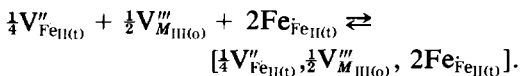


(3) diffusion;

and for an inverse spinel where all vacancies are on octahedral sites, Step (2) is written:



When diffusion is the only controlling process, interfacial steps(1) and (2) are in quasi-equilibrium. In the case of a total ionization of defects, applying the mass action law to equilibria 2 and 3, and from the relation expressing the concentration and electroneutrality, we could relate the concentration in Fe_{FeII} to the gas pressure (24). Calculation gives $[Fe_{FeII}] = k P_{O_2}^{2/11}$ whether the spinel is normal or inverse. In contrast, if we consider that the defects do not remain isolated without association, but that electrostatic interactions exist between charged species, equilibria 2 and 3 can be largely displaced by this association. For example, for a total association of vacancies and positive holes trapped on $Fe_{FeII(i)}$ or $Fe_{FeII(o)}$ sites, the step of the neutral diffusing defect, for equilibrium 2, is written:



Neglecting the concentration in free vacancies vs associated vacancies the mass action law gives:

$$K P_{O_2}^{1/2} = [\frac{1}{4} V''_{FeII(i)}, \frac{1}{2} V'''_{M_{III(i)}}, 2 Fe_{FeII(i)}].$$

Assuming such an association, we have shown (19) that, considering an isotropic medium in thermal equilibrium, it is possible to relate the expression of the oxidation rate to that of the concentration of associated vacancies from the rate equation of the various elementary steps. We obtain $v = k C$, where k is the rate constant and C the concentration in associated defects. The assumption of a strong association is fairly well verified by experiments since the study of the oxidation rate variation vs oxygen pressure given a law $P_{O_2}^{1/2}$ (Fig. 6). However, for zinc highly substituted magnetites where the defect concentration is far less and where association phenomena are less liable to occur, we actually find for the pressure law a far lower exponent (Fig. 6) since it is close to $\frac{1}{2}$.

These kinetic results suggest that the decrease in the chemical diffusion coefficient with the increase in vacancy extent and the exponent of the pressure law $P_{O_2}^{1/2}$ for defect phases substituted by trivalent ions or slightly substituted by divalent ions are explained by a vacancy-positive-charge association. Alternatively, the γ phases, whose substitution extent in divalent ions is high and which thus have few

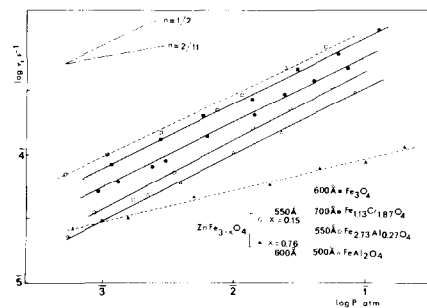


FIG. 6. Pressure law in the oxidation of different spinels.

vacancies, have a constant chemical diffusion coefficient for any α and may be considered as deprived of electrostatic interactions between defects.

Influence of Defects on Electrical Conductivity

The results obtained during the study of electrical properties (25) all confirmed Verwey's theory (26) interpreting the high conductivity of pure magnetite by the possible electron "hopping" between Fe^{2+} and Fe^{3+} ions present both on equivalent sites, here octahedral sites. Indeed, we have observed, for magnetites slightly substituted by trivalent ions and for magnetites substituted by divalent ions a high conductivity due to the presence of Fe^{3+} and Fe^{2+} ions on octahedral sites. This possibility of "hopping" has also been observed on tetrahedral sites during the oxidation of direct spinels (27) which, initially, only contain Fe^{2+} ions on these sites but which have both Fe^{2+} and Fe^{3+} ions during oxidation. Figure 7 shows these different possibilities of "hopping" according to the nature of the spinel and as a function of oxidation extent. It is noticed that only direct and totally oxidized spinels no longer show this "hopping" possibility and hence have a low conductivity. It thus appears that the vacancies generated during oxidation affect largely the electrical properties of these compounds. Let us give several examples where the electrical behavior during oxidation is related to the presence of vacancies.

1. Evolution of Conductivity with Time during the Oxidation of Inverse Spinel

Inverse spinels like magnetites substituted by trivalent ions ($x < 0.80$) or spinels substituted by divalent ions show a large decrease in conductivity during oxidation due to the occurrence of vacancies on octahedral sites which upset the electron "hopping" $Fe^{2+}-Fe^{3+}$. We have, for a given

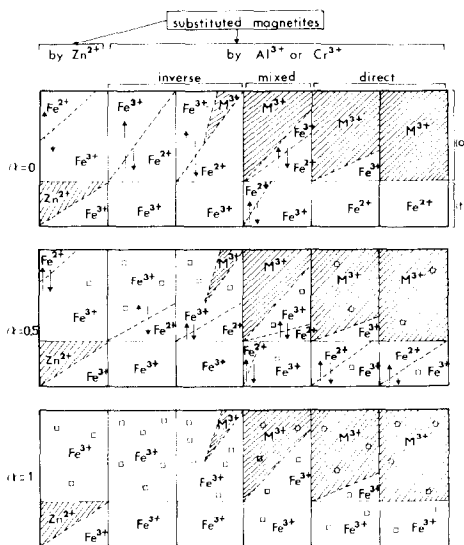


FIG. 7. Scheme of the various $Fe^{2+}-Fe^{3+}$ "hopping" possibilities ($\uparrow\downarrow$). \square : vacancies.

composition, recorded this conductivity decrease vs time. From these data we have plotted the $\alpha = f(t)$ curve, α being the transformation extent defined by $\alpha = (\sigma_0 - \sigma_t) / (\sigma_0 - \sigma_f)$, where

σ_0 is the conductivity in vacuum at the given temperature;
 σ_t is the conductivity at time t ; and
 σ_f is the conductivity of the γ phase (totally oxidized product).

The curves are reported in Fig. 8. They are practically similar to the $\alpha = f(t)$ curves obtained in thermogravimetry by recording the weight gain corresponding to oxygen fixation. In particular, they are practically superposable whatever the composition. Thus we can deduce that the weight change recorded in the thermobalance is equivalent to the conductivity change resulting from the introduction of vacancies on octahedral sites.

2. Case of Direct Spinel

Such an analogy between the kinetic curves is not found for magnetites highly substituted by trivalent ions or for chro-

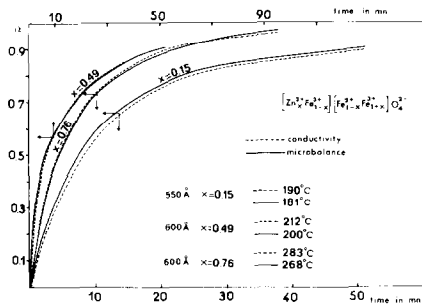


FIG. 8. Analogy between the $\alpha = f(t)$ curves obtained by thermogravimetry and by electrical conductivity.

mialuminates of iron II for, in this case, an initial conductivity increase is observed due to the formation through oxidation of Fe^{3+} ions on tetrahedral sites which favors electron "hopping" on these sites (Fig. 9). Thus, when the amount of Fe^{3+} ions is large, the "hopping" is upset by the vacancies which, as shown, are also present on tetrahedral sites and conductivity decreases as for inverse spinels.

Maximum conductivity increases approximately when $\alpha = 0.5$, i.e., when the amount of Fe^{2+} and Fe^{3+} ions on tetrahedral sites is equivalent. To verify this we have studied oxidation vs time for various, already partially oxidized spinels and whose oxidation extent is known. As can be noticed in Fig. 10 conductivity increases initially vs time if $\alpha < 0.5$ and it decreases from the very beginning if $\alpha > 0.5$. In the latter case, the behavior is similar to that of inverse spinels, where a sharp conductivity decrease is observed from the beginning of oxidation.

3. Electrical Conductivity of Magnetites Slightly Oxidized near the Verwey Transition Temperature

At low temperature, magnetites slightly Al or Cr substituted ($x < 0.27$) and slightly oxidized ($\delta < 0.040$) show a break and also a change in the slope of the $\log \sigma = f(t)$ curves. This phenomenon, observed by

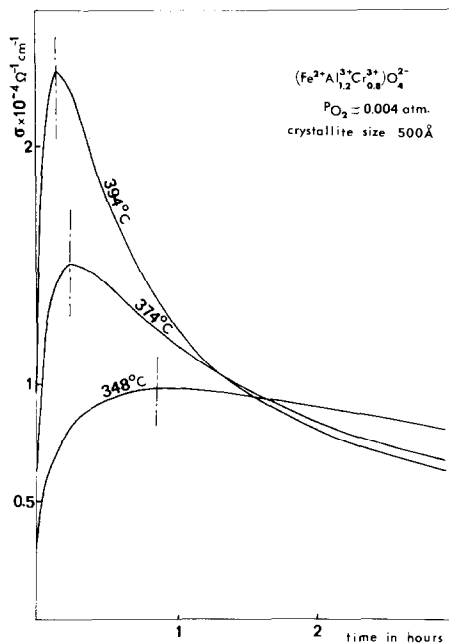


FIG. 9. Evolution of conductivity vs time for different oxidation temperatures of direct spinels.

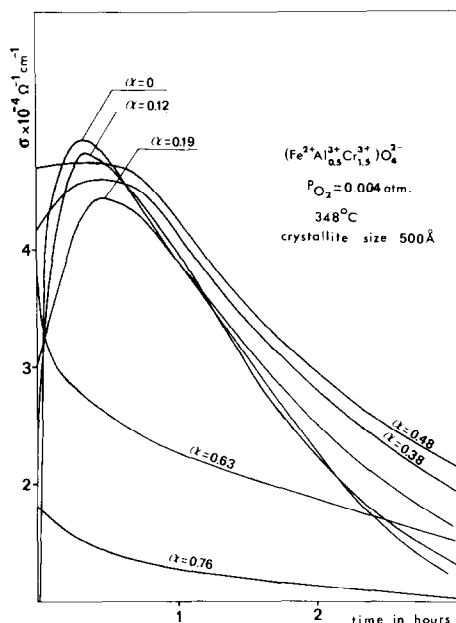


FIG. 10. Evolution of conductivity vs time for different oxidation extents α .

Verwey for pure magnetite (26), is attributed to the crystallographic transition of magnetite at 119°K and is explained by the creation of an order between Fe²⁺ and Fe³⁺ ions in the layers perpendicular to the (001) axis. Figure 11 shows that temperature and the magnitude of the Verwey transition decrease with x and δ . In addition, conductivity changes differently depending on whether we are in a temperature range higher or lower than the transition temperature T_1 . For temperature above T_1 conductivity decreases either with the substitution extent in trivalent ions or with the vacancy extent. Alternatively, for temperatures below T_1 slightly oxidized magnetite shows a higher conductivity than pure magnetite, but only if δ is less than 0.040.

The model of double exchange recently developed (28) explains the conductivity decrease with x and δ for temperatures above T_1 considering that the introduction of foreign cations or of vacancies on octahedral sites disturb electron "hopping." Below T_1 the crystallographic change of the cubic symmetry into a symmetry lower than orthorhombic is reported in Figure 12a with the octahedral cations Fe²⁺ and Fe³⁺ on alternate (001) planes. This arrangement shows that double "hopping" is less liable here than in magnetite above T_1 , since electron "hopping" is only possible between the (001) planes and no longer occurs inside these planes given that they contain

iron ions of the same valence. This decrease will still be greater during substitution since electron "hopping" between the (001) planes will be more difficult because of the presence of M³⁺ ions (Fig. 12b).

Now if we consider slightly substituted magnetite we see that conductivity is higher than that of pure magnetite. Following the oxidation reaction, 3Fe²⁺ → 2Fe³⁺ + □ we see that if 3Fe²⁺ is replaced by 2Fe³⁺ and a vacancy in the scheme of Fig. 12a, we come to the case reported in Fig. 12c. We then observe that, inside the (001) planes, electron "hopping" can still occur, which results in a conductivity increase as observed experimentally. For high values of nonstoichiometry ($\delta > 0.040$) or for slightly substituted and oxidized magnetites (Fig. 12d), conductivity is lower than for magnetite oxidized up to $\delta = 0.025$ and, at the same time, the break in the transition temperature disappears. In these conditions a too large number of unequivalent sites inside the (001) planes cancels the

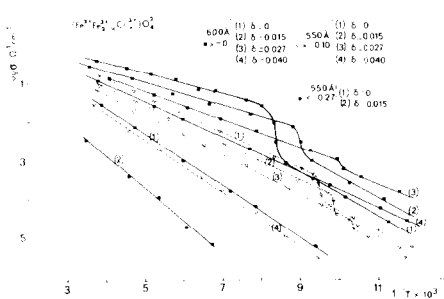


FIG. 11. Variation in the electrical conductivity logarithm with inverse temperature with x and δ .

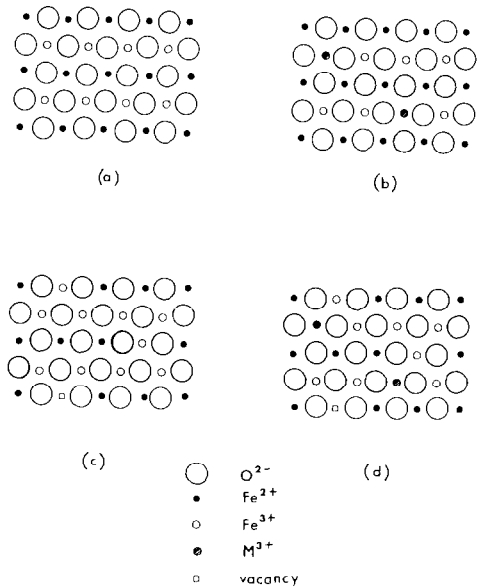


FIG. 12. Representation along two directions of the octahedral sublattice of pure or nonstoichiometric magnetite below transition temperature T_1 .

electron "hopping" process. In addition, as the transition temperature is related to the occurrence of an ordering between Fe^{2+} and Fe^{3+} ions (29) we observe in all cases a decrease in this transition temperature with ordering collapse by introduction of an foreign element (atom or vacancy).

Conclusion

These results show that in the system considered here, which are all of type $S_1 + G = [S_1 + d]$, where $[S_1 + d]$ is the metastable phase of spinel structure enriched in defects, the knowledge of the concentration and location of vacancies generated during oxidation allows us to interpret most of the kinetic and electrical conductivity results. The various discussions reported in this study show that elaborate experimental studies are required with well-defined products, as well as intermediate states of known composition, the vacancy distribution of which is compatible with the lattice parameters so as to enable us to decide between the different hypotheses put forward and validate or invalidate the criteria obtained by comparison with $\gamma\text{Fe}_2\text{O}_3$.

Finally, it should be recalled, still by analogy with $\gamma\text{Fe}_2\text{O}_3$, that these defect phases must be considered as an intermediate monophasic state with an extended homogeneity domain from which a solid phase of different structure can precipitate. In this case, the process of structural rearrangement still involves the elimination and migration of vacancies under cooperative movements (30, 31).

References

1. B. GILLOT, A. ROUSSET, AND G. DUPRE, *J. Solid State Chem.* **25**, 263 (1978).
2. A. ROUSSET, P. MOLLARD, AND A. GIRAUD, *C.R. Acad. Sci. (Paris) Ser. C* **275**, 709 (1972).
3. A. ROUSSET, J. PARIS, AND P. MOLLARD, *Ann. Chim. Fr.* **7**, 119 (1972).
4. A. ROUSSET, F. CHASSAGNEUX, AND P. MOLLARD, *C.R. Acad. Sci. (Paris) Ser. C* **279**, 1129 (1974).
5. G. DUPRE, A. ROUSSET, AND P. MOLLARD, *Mater. Res. Bull.* **11**, 473 (1976).
6. B. GILLOT, J. TYRANOWICZ, AND A. ROUSSET, *Mater. Res. Bull.* **10**, 775 (1975).
7. B. GILLOT, J. F. FERRIOT, G. DUPRE, AND A. ROUSSET, *Mater. Res. Bull.* **11**, 843 (1976).
8. B. GILLOT, F. BOUTON, F. CHASSAGNEUX, AND A. ROUSSET, *Mater. Res. Bull.* **15**, 1 (1980).
9. B. GILLOT AND F. BOUTON, *J. Solid State Chem.* **32**, 303 (1980).
10. B. GILLOT, *Mater. Res. Bull.* **13**, 783 (1978).
11. B. GILLOT, J. F. FERRIOT, AND A. ROUSSET, *J. Phys. Chem. Solids* **37**, 857 (1976).
12. P. POIX, *Sémi. Chim. l'Etat Solide* **1**, 82 (1966-1967).
13. R. DIECKMANN, *Z. Phys. Chem. N. F.* **107**, 189 (1977).
14. P. POIX, "Liaisons interatomiques et propriétés physiques des composés minéraux, p. 82, SEDES, Paris (1968).
15. G. J. KOEL AND P. J. GELLINGS, *Oxid. Metals* **5**, 185 (1972).
16. P. E. CHILDS, L. W. LAUB, AND J. B. WAGNER, *Proc. Brit. Ceram. Soc.* **19**, 29 (1971).
17. R. DIECKMANN AND H. SCHMALZRIED, *Ber. Bunsen Ges. Physik. Chem.* **81**, 414 (1977).
18. A. NAKAMURA, S. YAMAUCHI, K. FUEKI, AND T. MUKAIBO, *J. Phys. Chem. Solids* **39**, 1203 (1978).
19. B. GILLOT, D. DELAFOSSE, AND P. BARRET, *Mater. Res. Bull.* **8**, 1431 (1973).
20. K. J. GALLAGHER, W. FEITKNECHT, AND U. MANNWEILLER, *Nature* **217**, 1118 (1968).
21. R. L. LEVIN AND J. B. WAGNER, JR., *Trans. Met. Soc. AIME* **233**, 159 (1965).
22. J. P. PRICE, Ph. D. Thesis, Northwestern Univ. Evanston, Ill (1968).
23. A. KRÖGER AND H. J. VING, "Solid State Physics," Vol. 3, p. 307, Academic Press, New York, (1956).
24. B. GILLOT, *Mater. Res. Bull.* **1**, 31, (1980).
25. B. GILLOT, *J. Phys. Chem. Solids* **38**, 751 (1977).
26. E. J. W. VERWEY AND P. W. HAAYMAN, *Physica* **8(9)**, 979 (1941).
27. B. GILLOT, F. BOUTON, F. CHASSAGNEUX, AND A. ROUSSET, *Phys. Status Solidi A* **50**, 109 (1978).
28. B. GILLOT, *J. Phys. Chem. Solids* **40**, 261 (1979).
29. L. R. BICKFORD, J. M. BROWNLOW, AND R. F. PENOYER, *Proc. Inst. Elec. Engrs. Lond B* **104**, 238 (1957).
30. B. GILLOT, F. BOUTON, F. CHASSAGNEUX, AND A. ROUSSET, *J. Solid State Chem.* **33**, 245 (1980).
31. S. KACHI, K. MOMIYAMA, AND S. SHIMIZU, *J. Phys. Soc. Japan*, **1**, 18 (1963).